The Formation of Chondrules at High Gas Pressures in the Solar Nebula

Albert Galy,*† Edward D. Young, Richard D. Ash, R. Keith O'Nions

High-precision magnesium isotope measurements of whole chondrules from the Allende carbonaceous chondrite meteorite show that some aluminum-rich Allende chondrules formed at or near the time of formation of calcium-aluminum–rich inclusions and that some others formed later and incorporated precursors previously enriched in magnesium-26. Chondrule magnesium-25/magnesium-24 correlates with [magnesium]/[aluminum] and size, the aluminum-rich, smaller chondrules being the most enriched in the heavy isotopes of magnesium. These relations imply that high gas pressures prevailed during chondrule formation in the solar nebula.

Chondritic meteorites are composed largely of mm-sized objects such as chondrules and Ca-Al–rich inclusions (CAIs). Chondrules and many CAIs formed by the rapid cooling of droplets of molten or partially molten rock in space (*1*). These small objects are bound within a matrix composed of a complex mixture of μm-scale silicate, oxide, and sulfide grains as well as reduced carbon compounds. The timing, duration, and conditions of CAIs and chondrule formation remain poorly constrained. These objects formed in the solar nebula before their accretion into the parent body of the chondritic meteorites and therefore bear witness to the conditions that prevailed in the solar nebula (*1*). However, this record of the solar nebula may have been partly erased by the complex history of the meteorite parent bodies, which includes collision-induced shock, thermal metamorphism, and aqueous alteration (*1*).

Magnesium isotopes are useful for reconstructing the history of the solar nebula. The short-lived nuclide ^{26}Al [half-life = 0.73 million years (My)] decays to ^{26}Mg, providing a high-resolution relative chronometer. The partitioning of Mg isotopes according to mass during many physicochemical processes, including evaporation of molten rock at subatmospheric pressures, is large enough to be measurable (*2*). CAIs are the oldest, most primitive remains of the primordial solar nebula, and an initial ^{26}Al/^{27}Al value of 5×10^{-5} at the time of their formation has been inferred on the basis of excesses in ^{26}Mg (^{26}Mg*) relative to mass-dependent variations in Mg isotope ratios. ^{26}Mg* is attributed to decay of ^{26}Al because it correlates with the concentration of Al (*3*). Except for a few Al-rich chondrules from various chondrites, including Allende, most chondrules have no resolvable ^{26}Mg* (*4*). In these Al-rich chondrules, initial ^{26}Al/^{27}Al [(^{26}Al/^{27}Al)$_0$] values of 0.6×10^{-5} are obtained from intrachondrule isochrons (*5*). The difference in (^{26}Al/^{27}Al)$_0$ between CAIs and chondrules has been attributed to chondrule formation beginning >2 My after CAIs and continuing for at least another 5 My (*6*). Although mass-dependent variations in ^{25}Mg/^{24}Mg, ^{26}Mg/^{24}Mg, ^{29}Si/^{28}Si, and ^{30}Si/^{28}Si in CAIs indicate evaporation of these materials in the early solar nebula (*2*), isotopic evidence for evaporation in chondrules or chondrule precursors has not yet been described (*7*).

Here, we report measurements of the Mg-isotopic abundances and Mg/Al of bulk chondrules and a CAI from the Allende carbonaceous chondrite meteorite (Table 1). Measurements of ^{25}Mg/^{24}Mg and ^{26}Mg/^{24}Mg in whole chondrules can simplify the interpretation of the data relative to single mineral analyses because it is insensitive to the migration of elements within individual chondrules (*8*, *9*) subsequent to their formation. However, whole-chondrule isotopic abundances may also be affected by inheritance from chondrule precursors (*10*). High-precision Mg-isotopic abundances were obtained by multicollector inductively coupled mass spectrometry (MC-ICPMS) (*11*, *12*). This method increases the precision by at least an order of magnitude relative to other techniques (*2*) and makes possible comparisons between bulk chondrules, chondrite matrix, and terrestrial materials.

The Mg-isotopic abundances of terrestrial materials define a single mass fractionation curve on a Mg three-isotope plot (Fig. 1), termed the terrestrial fraction curve (TF). The bulk composition of Allende, its matrix, and ferromagnesian chondrules exhibit no resolvable ^{26}Mg* with respect to terrestrial material. Two of the 14 chondrules analyzed (A4 and AH2, Table 1) lie off the TF (Fig. 1), with ^{26}Mg* values of 0.23 and 0.15 per mil (‰), respectively. Both chondrules with resolvable ^{26}Mg* are Al-rich (Fig. 1). Model isochrons (which assume terrestrial ^{26}Mg* for the low-Al phase) give (^{26}Al/^{27}Al)$_0$ ratios of $(1.86 \pm 0.73) \times 10^{-5}$ and $(3.70 \pm 1.21) \times 10^{-5}$ for A4 and AH2, respectively (Fig. 2). The CAI exhibits a ^{26}Mg* value of 2.03‰, and a model isochron yields (^{26}Al/^{27}Al)$_0$ ratio $(6.24 \pm 0.23) \times 10^{-5}$, in agreement with the highest (^{26}Al/^{27}Al)$_0$ previously found in CAIs (*4*).

The highest chondrule (^{26}Al/^{27}Al)$_0$ value is six times higher than those previously reported for Allende chondrules (*5*) and is within the range for many CAIs from carbonaceous chondrites (*4*, *13*). The bulk ^{26}Mg* in the Al-rich chondrules and the CAI may be interpreted in two ways. If an object is a direct condensate, then its bulk excesses in ^{26}Mg reflect its relative age of formation. If, on the other hand, the objects inherited ^{26}Mg* and/or its parent ^{26}Al from precursor solids, then the bulk values provide no relative age information and are instead an indication of the degree of mixing. In the case of most of our chondrules, including AH2, mixing between chondritic material and CAIs can explain the data (Figs. 2 and 3). Late formation of chondrules and incorporation of varying amounts (between 0 and 17%) of pieces of CAIs are consistent with the interpretation of rare earth element patterns in chondrules (*14*). In the case of chondrule A4, mixing between CAIs and chondritic material is not able to explain the data. Mixing would require a third component that was rich in Al but with little ^{26}Mg* or ^{26}Al. If ^{26}Mg* in A4 is the result of the decay of ^{26}Al incorporated during the chondrule formation and not mixing, it would imply that A4 formed 1.4 (+0.7, −0.5) My after the formation of the most primitive CAIs, assuming a homogeneous (^{26}Al/^{27}Al)$_0$ in the solar nebula (*15*), reducing the time interval between CAIs (*13*) and the onset of chondrule formation from the previous estimate of 2 My (*6*) to 1 My.

Correspondence between δ^{25}Mg of Allende matrix and normal ferromagnesian chondrules supports a well-mixed Mg reservoir for the Allende parent body. The rim and core subfractions of a single chondrule with a thick rim (Table 1) are similar in δ^{25}Mg and δ^{26}Mg, suggesting that the different δ^{25}Mg values between chondrules are not the result of the presence or absence of a rim. Where δ^{25}Mg and δ^{26}Mg do vary, the variations correlate with Mg/Al, the Al-rich chondrules being the most enriched in heavy isotopes (Fig. 3). In addition, a systematic inverse relation has been found between the size of the chondrules (estimated from their masses, Table 1) and δ^{25}Mg (*12*).

Correlations between Mg isotope ratios, Mg/Al, and size constrain the conditions attending early formation of the Allende chondrules because equilibrium vapor pressures for silicate liquids exceed most estimates for ambient gas pressures in the early solar neb-

---

Department of Earth Sciences, University of Oxford, Parks Road, Oxford, OX1 3PR, UK.

*To whom correspondence should be addressed. E-mail: albert00@esc.cam.ac.uk

†Present address: Department of Earth Sciences, University of Cambridge, Downing Street, Cambridge, CB2 3EQ, UK.

Table 1. Al-Mg isotopic data for Allende matrix and chondrule.

Sample	Type	Description*	Mass (mg)	$^{27}Al/^{24}Mg$‡	$\delta^{26}Mg$§ (‰)	2σ	$\delta^{25}Mg$§ (‰)	2σ	$\Delta^{26}Mg$‖ (‰)	2σ
AG22				0.122	3.13	0.04	1.59	0.03	0.01	0.02
AG22	Dupl. 1			nd	3.14	0.07	1.60	0.04	0.02	0.01
AG22	Dupl. 2			nd	3.07	0.09	1.57	0.06	0.01	0.06
AG22	Average	Bulk†		0.122	3.12	0.07	1.59	0.03	0.01	0.03
AG23				0.128	3.11	0.04	1.59	0.01	0.00	0.04
AG23	Dupl. 1			nd	3.14	0.04	1.60	0.03	0.02	0.04
AG23	Average	Matrix†		0.128	3.13	0.04	1.60	0.01	0.01	0.00
AG38	Chond.	nd	41.92	0.089	3.08	0.09	1.57	0.04	0.02	0.04
A1	Chond.	nd	7.65	0.087	3.36	0.03	1.72	0.02	0.00	0.00
A2	Ch.+Rim	RP	11.08	0.140	3.77	0.13	1.93	0.07	0.00	0.01
A3	Chond.	POP	17.68	0.078	3.17	0.06	1.63	0.06	−0.02	0.09
A4	Chond.	Al-rich	2.22	1.708	5.07	0.08	2.49	0.07	0.23	0.11
A5	Chond.	POP	2.75	0.334	3.91	0.05	1.97	0.08	0.06	0.22
A6	Chond.	PO	13.53	0.263	3.80	0.12	1.94	0.06	0.00	0.00
A7	Ch.+Rim	BO	12.36	0.087	3.16	0.03	1.63	0.02	−0.02	0.00
A8	Ch.+Rim	nd	30.07	0.115	3.05	0.11	1.57	0.04	−0.02	0.08
AH1	Chond.	P?	13.51	0.325	3.84	0.04	1.94	0.00	0.06	0.08
AH2	Ch.+Rim	nd	10.79	0.575	5.24	0.02	2.61	0.02	0.15	0.04
AH3	Ch.+Rim	P?	13.32	0.134	3.22	0.04	1.66	0.02	−0.02	0.00
AH4	Chond.	P?	8.06	0.308	4.06	0.03	2.04	0.05	0.08	0.12
A9	Rim	nd		0.170	3.30	0.04	1.69	0.02	0.00	0.03
A9	Core	nd		0.184	3.43	0.04	1.75	0.03	0.01	0.02
AG178	CAI	nd	2.64	4.547	15.37	0.02	6.87	0.01	2.03	0.03

*RP, radial pyroxene; POP, porphyric olivine pyroxene; Al-rich, aluminum-rich mineralogy; PO, porphyric olivine; BO, barred olivine; P?, porphyric; nd, not determined. †Bulk and matrix fraction are size fractions (<48 μm and <20 μm) described in (*27*). ‡The Al/Mg has been measured by MC-ICPMS, and the uncertainty is 2% relative. §Mg-isotopic compositions are expressed as a per mil deviation from the isotopic composition of the international standard SRM 980 (*28*) as follows: $\delta^{x}Mg = [(^{x}Mg/^{24}Mg)_{Sample}/(^{x}Mg/^{24}Mg)_{SRM980} - 1] \times 1000$. ‖The excess of ^{26}Mg, $\Delta^{26}Mg$, is the per mil deviation from the TF (Fig. 1) and is calculated by the relation $\Delta^{26}Mg = \delta^{26}Mg - [(1/0.5163) \times (\delta^{25}Mg + 0.015)]$, where 0.5163 is the slope of the TF and −0.015 is the *y* axis intercept (determined on 61 terrestrial samples, with a $\delta^{26}Mg$ range of 5.3‰).

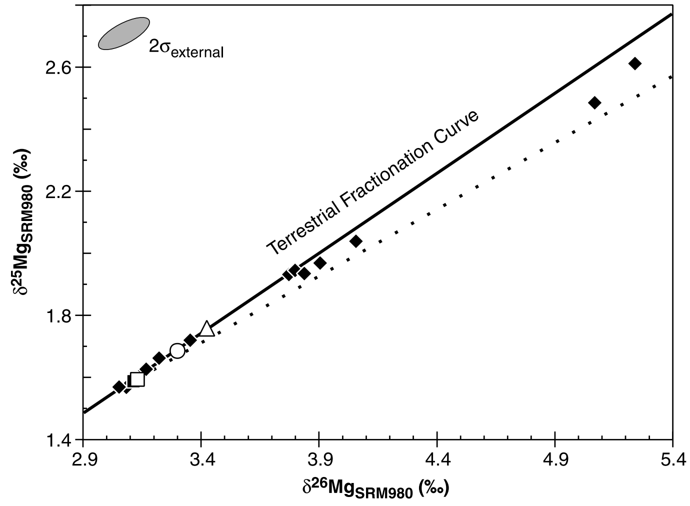

Fig. 1. Three-isotope plot for magnesium in Allende meteorite material. The black square corresponds to the bulk composition of the Allende meteorite, the open square to the matrix, and the diamonds to the chondrules. The open circle and triangle represent the rim and the core of a single chondrule having a large rim (Table 1). The terrestrial fractionation curve (TF) is defined by 61 samples from various geological or biological environments. The gray ellipse [95% confidence interval (2σ) on duplicate chemistry separation and mass spectrometry measurement] gives the uncertainty for the measurements. The dotted line corresponds to the mixing line between the matrix or the biggest chondrule and the measured CAI (CAI is off scale to the right). Within errors, all the Allende material, except two chondrules, lie on the TF.

ula (*16*, *17*) and the chondrules are expected to have evaporated as they floated in a molten state in space. The relations between size, Mg/Al, and $^{25}Mg/^{24}Mg$ and $^{26}Mg/^{24}Mg$ in the chondrules are consistent with evaporation during formation.

On the basis of the assumption that the initial chemical and isotopic compositions of the chondrules were similar, we modeled the evolution of Mg/Al, $^{25}Mg/^{24}Mg$, and $^{26}Mg/^{24}Mg$ during evaporation of a molten chondrule. The calculations are based on a physical model for evaporation that accounts for the partition coefficients of Mg and Al between liquid and vapor, the rate of diffusion of Mg and Al within the volatilizing liquid, and the reduction in size of the chondrule as it loses mass (*18*, *19*).

Results of the calculations show that correlation between Mg/Al, $\delta^{25}Mg$, and total mass among the chondrules can be explained by evaporation if the diffusive-evaporative Peclet number for Mg, β [defined as $r(dr/dt)/D$, where r is the radius of the spherical chondrule, t is time, and D is the diffusion coefficient for Mg], is on the order of 300 ± 100 (Fig. 3). This value for the Peclet number is >100 times larger than the values obtained in laboratory experiments for free evaporation of molten silicates with sizes comparable to chondrules (*2*). There are two explanations for such high values for β during evaporation. One is that the Al-rich chondrules were larger (30 cm in diameter) before evaporation. Such large sizes are inconsistent with the observation that the least evolved chondrules (lowest Al/Mg) have radii <1 cm, so this hypothesis can be rejected. The alternative explanation is that the rate of evaporation was accelerated by high ambient gas pressures relative to canonical estimates for pressures (P) in the inner solar nebula ($P = 0.1$ to 100 Pa) (*20*). The isotopic effects of evaporation are reduced when the rate of evaporation exceeds the free evaporation rate by a factor of 100 or more, which occurs in the laboratory when ambient pressures approach 1 atmosphere (*21*, *22*) ($P >$ 100 Pa). The effect is particularly striking when the ambient gas phase is dominantly H_2 (*21*).

The constraint of high β can be relaxed ($\beta <$ 100) if it is assumed that the isotopic fractionation was not related to the kinetics of volatilization but instead was controlled by an approach to thermodynamic equilibrium at high temperature where isotope fractionation is minimal. For example, the data can be fit with $\beta = 1.33$, consistent with experimental data for free evaporation of forsterite liquid (*18*), if the $^{25}Mg/^{24}Mg$ in volatil-

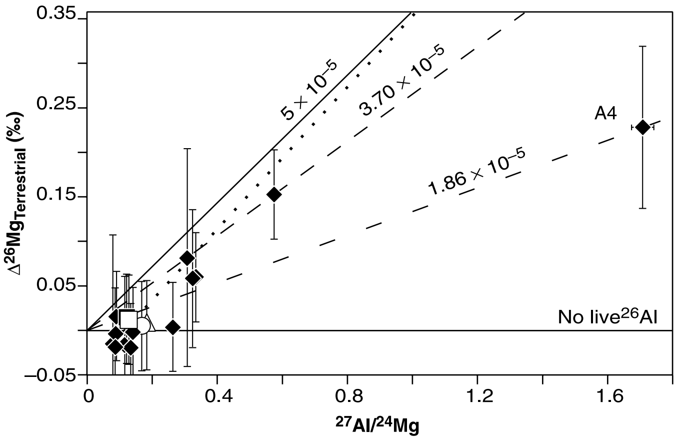

Fig. 2. Al-Mg evolution diagram. Symbols are the same as those in Fig. 1. The error bars are the larger of either 2σ external (0.05‰) or 2σ measured (Table 1). The dotted line corresponds to the mixing line between the matrix and the measured bulk CAI (off scale). With respect to Al and Mg, the chemical composition of the matrix is chondritic. Our measurement of the Mg-isotopic abundance of a bulk CAI is insensitive to late thermal resetting and, therefore, should be representative of CAIs. The two dashed lines are isochrons for the Al-rich chondrules.

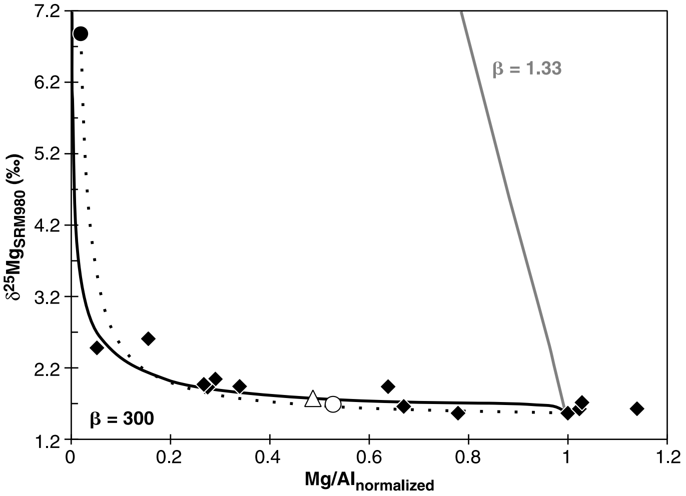

Fig. 3. Mg-isotopic composition versus Mg/Al normalized to the Mg/Al the biggest chondrule in this study (AG38, Table 1) for Allende chondrules and the CAI (solid circle) compared with calculated evolution during volatilization (solid curve) and mixing between the matrix and the measured CAI (dotted curve). Other symbols are the same as in Fig. 1. The curve for a Peclet number (β) of 1.33 represents free evaporation at low pressures ($P < 0.1$ Pa) (*18*). A high Peclet number suggests evaporation at higher pressures ($P > 100$ Pa) (*21*, *22*) during chondrule formation.

ized gas to that in the condensed phase was 0.9990 rather than the value of 0.9798 applicable to a purely kinetic process. In this case, enrichment in rock-forming elements in the gas phase relative to canonical solar gas compositions is implied because the partial pressure of Mg would have to have approached the equilibrium vapor pressure for silicate liquid. Equilibrium between chondritic melts and vapor requires Mg enrichments of 12 times to >400 times relative to solar compositions at early solar nebula total pressures of 100 Pa (*18*). A similar conclusion has been drawn from the lack of K-isotopic variations in chondrules (*7*, *23*). However, if an increase of two orders of magnitude relative to solar compositions of the partial pressure for highly volatile elements (K) is plausible, it is less likely for less volatile elements (Mg). Therefore, Mg-isotopic abundances in chondrules suggest a high total gas pressure. Whether this environment was very localized or corresponds to the condition prevailing in a large portion of the solar nebula remains unsolved.

Under high gas pressures, the chemical and isotopic compositions of molten materials are barely influenced by volatilization. In this case, variability in Mg/Al, $^{25}Mg/^{24}Mg$, and $^{26}Mg/^{24}Mg$ in chondrules from an individual meteorite is not the result of the chondrule-forming process but instead reflects heterogeneous starting materials. Except for one (A4), our chondrule data can be explained by a binary mixture of chondritic-like material and CAI-like material (Figs. 2 and 3). Our study shows that chondrules formed at higher pressures relative to canonical solar nebula pressures and that some chondrules and CAIs formed penecontemporaneously. Among the various models proposed for chondrule formation, the timing and high pressures suggested by the bulk Mg-isotope data are consistent with the formation of chondrules in shock waves or as ejecta from collisions among young objects formed in the solar nebula (*16*).

References and Notes

1. R. H. Hewins, in *Chondrules and the Protoplanetary Disk*, R. H. Hewins, R. H. Jones, E. R. D. Scott, Eds. (Cambridge Univ. Press, Cambridge, 1996), pp. 3–9.
2. A. M. Davis, A. Hashimoto, R. N. Clayton, T. K. Mayeda, *Nature* **347**, 655 (1990).
3. T. Lee, D. A. Papanastassiou, G. J. Wasserburg, *Astrophys. J.* **211**, L107 (1977).
4. G. J. MacPherson, A. M. Davis, E. K. Zinner, *Meteoritics* **30**, 365 (1995).
5. Y. J. Sheng, I. D. Hutcheon, G. J. Wasserburg, *Geochim. Cosmochim. Acta* **55**, 581 (1991).
6. S. S. Russell, G. Srinivasan, G. R. Huss, G. J. Wasserburg, G. J. MacPherson, *Science* **273**, 757 (1996).
7. C. M. O'D. Alexander *et al.*, *Meteorit. Planet. Sci.* **35**, 859 (2000).
8. T. LaTourrette, G. J. Wasserburg, *Earth Planet. Sci. Lett.* **158**, 91 (1998).
9. F. A. Podosek *et al.*, *Geochim. Cosmochim. Acta* **55**, 1083 (1991).
10. R. D. Ash, A. Galy, E. D. Young, R. K. O'Nions, *Meteorit. Planet. Sci.* (suppl.) **35**, A21 (2000).
11. L. Halicz, A. Galy, N. S. Belshaw, R. K. O'Nions, *J. Anal. Atom. Spectrom.* **14**, 1835 (1999).
12. A. Galy, E. D. Young, R. D. Ash, R. K. O'Nions, *Lunar Planet. Sci.* **XXXI** (abstract 1193) (2000) [CD-ROM].
13. W. Hsu, G. J. Wasserburg, G. R. Huss, *Earth Planet. Sci. Lett.* **182**, 15 (2000).
14. K. Misawa, N. Nakamura, in *Chondrules and the Protoplanetary Disk*, R. H. Hewins, R. H. Jones, E. R. D. Scott, Eds. (Cambridge Univ. Press, Cambridge, 1996), pp. 99–105.
15. Among all the classes of meteorites where CAIs are present, most of the highest $(^{26}Al/^{27}Al)_0 \sim 5 \times 10^{-5}$, suggesting a widespread and uniform occurrence of ^{26}Al when CAIs started to form (*4*, *6*). However, CAIs do not sample the entire solar nebula, and the ^{26}Al could have been produced by cosmic-ray irradiation of the CAI precursors (*24*), as suggested by the presence of spallogenic-produced ^{10}Be in Allende CAIs (*25*). Those models already suggest a contemporaneous formation for chondrules and CAIs, and to support our conclusion, we used a less favorable hypothesis (*6*) to look at the time difference between CAIs and chondrules.
16. A. P. Boss, in *Chondrules and the Protoplanetary Disk*, R. H. Hewins, R. H. Jones, E. R. D. Scott, Eds. (Cambridge Univ. Press, Cambridge, 1996), pp. 257–264.
17. D. S. Ebel, L. Grossman, *Geochim. Cosmochim. Acta* **64**, 339 (2000).
18. E. D. Young, H. Nagahara, B. O. Mysen, D. M. Audet, *Geochim. Cosmochim. Acta* **62**, 3109 (1998).
19. In these calculations, estimates for the partitioning of Mg and Al between liquid and vapor were obtained from experimental data (*26*) and are 0.7 and 0.02, respectively. Differences in $^{25}Mg/^{24}Mg$ (and $^{26}Mg/^{24}Mg$) between liquid and vapor were prescribed by kinetic isotopic fractionation factors [e.g., $\sqrt{24/25}$ for δ^{25}Mg (*3*)].
20. J. A. Wood, G. E. Morfill, in *Meteorites and the Early Solar System*, J. F. Kerridge, M. S. Matthews, Eds. (Univ. of Arizona Press, Tucson, AZ, 1988), pp. 329–347.
21. H. Nagahara, K. Ozawa, *Geochim. Cosmochim. Acta* **60**, 1445 (1996).
22. F. M. Richter, N. Parsad, A. M. Davis, A. Hashimoto, *Lunar Planet. Sci.* **XXX** (abstract 1989) (1999) [CD-ROM].
23. P. Georges, G. Libourel, E. Deloule, *Meteor. Planet. Sci.* **35**, 1183 (2000).
24. D. D. Clayton, L. Jin, *Astrophys. J.* **451**, L87 (1995).
25. K. D. McKeegan, M. Chaussidon, F. Robert, *Science* **289**, 1334 (2000).
26. C. Floss *et al.*, *Geochim. Cosmochim. Acta* **60**, 1975 (1996).
27. J. W. Arden, *Earth Planet. Sci. Lett.* **62**, 395 (1983).
28. E. J. Catanzaro, T. J. Murphy, E. L. Garner, W. R. Shields, *J. Natl. Bur. Stand.* **70A**, 453 (1966).
29. We thank N. S. Belshaw for his expertise in mass spectrometry. The constructive comments by two anonymous reviewers and various discussions with S. S. Russell and M. Chaussidon are highly appreciated. Supported by a grant from the Particle Physics and Astronomy Research Council, UK (PPA/G/S/1998/00069) to E.D.Y.

4 August 2000; accepted 20 October 2000